J Ther Eng, Vol. 11, No. 2, pp. 344−356, March, 2025

Journal of Thermal Engineering
Web page info: https://jten.yildiz.edu.tr
DOI: 10.14744/thermal.0000919

Research Article

Unsteady magnetohydrodynamic free convection flow of Al_2O_3–Cu/water nanofluid over a permeable linear stretching sheet through a porous medium with viscous dissipation and heat source/sink

Joel MATHEWS[1,*], Hymavathi TALLA[2]

[1]*Department of Mathematics, Krishna University, Machilipatnam, 521004, India*
[2]*Department of Mathematics, Adikavi Nannaya University, University College of Science and Technology, Rajamahendravaram, 533296, India*

ARTICLE INFO

Article history
Received: 13 April 2024
Revised: 23 July 2024
Accepted: 24 July 2024

Keywords:
Heat Source/Sink; Magnetohydrodynamics (MHD); Nanofluids; Permeable Sheet; Thermal Radiation; Viscous-dissipation

ABSTRACT

This paper examines the effect of Copper and Aluminium oxide nanoparticles on the MHD water-based flow over a permeable linearly stretching sheet through a porous medium. The objective of the present work is to exhibit the impact of magnetic field, viscous dissipation, thermal radiation, and heat source/sink with the metallic and oxide nanoparticles due to permeable stretching sheet. The significance of a new advanced nanofluid with two kinds of nanoparticle materials (Copper and Aluminium oxide) stems from the fact that in the design of various equipment, such as nuclear power plants, gas turbines, propulsion devices for aircraft, missiles, etc. Similarity variables were used to transform the nonlinear partial differential equations into ordinary differential equations. To solve the obtained ODEs, the MATLAB bvp4c solver is used. The behavior of velocity and temperature profiles is discussed through graphs. Also, the physical quantities, such as Skin friction coefficient and Nusselt number, for both fluids are calculated and presented via tables. We have compared the velocity profiles of nanofluids and pure fluid and observed that Copper and Alumina nanofluids perform more efficiently than the base fluid. Moreover, the numerical results are compared with the existing results and found to have good accuracy with the present results.

Cite this article as: Mathews J, Talla H. Unsteady magnetohydrodynamic free convection flow of Al_2O_3–Cu/water nanofluid over a permeable linear stretching sheet through a porous medium with viscous dissipation and heat source/sink. J Ther Eng 2025;11(2):344−356.

INTRODUCTION

The numerous industrial and engineering processes that involve boundary layer flow and heat transfer past a permeable linear stretching surface have piqued the interest of researchers. These operations include the fabrication and extraction of polymer and rubber sheets, among many others. The product's mechanical characteristics are determined by the stretching and cooling rates. The research on stretching sheet and boundary layer flow was first done

***Corresponding author.**
*E-mail address: lollajoel.mathews765@gmail.com

This paper was recommended for publication in revised form by Editor-in-Chief Ahmet Selim Dalkılıç

Published by Yıldız Technical University Press, İstanbul, Turkey
Yıldız Technical University. This is an open access article under the CC BY-NC license (http://creativecommons.org/licenses/by-nc/4.0/).

by Sakiadis [1, 2]. Under various conditions, the boundary layer flow across a continuous stretched sheet at a constant speed was examined. Crane [3] was the first among the others to consider an incompressible fluid flow due to a linearly stretching surface. The flow across a permeable shrinking/stretching sheet under different physical situations has been done by the following researchers. In 1977, Gupta and Gupta [4] extended Crane [3] work to heat and mass transfer flow when there is suction/injection. The MHD flow of a fluid with electrical conductivity by considering the larger values of the mass transfer parameter was given by Pop and Tsung [5]. Kumaran et al. [6] investigated how a conducting Newtonian fluid's boundary layer flows when a permeable sheet is involved. They discovered that stretching the sheet had a major impact on the streamlines. The MHD flow of a viscous fluid over a permeable shrinking sheet in the presence of prescribed surface heat flux is examined by Ali et al. [7]. Hayat et al. [8] investigated the fluid's heat transfer properties as it flows over a porous stretched surface during slip condition. Later, Mabood and Shateyi [9] examined the thermal radiation and multiple-slip effects on a permeable stretched sheet. On the other hand, flows in real-world systems are typically not steady because flow conditions change over time. Natural processes, human acts, or accidents and occurrences might be to blame for the unsteadiness. As a function of both space and time, the analysis of unsteady flows is often more involved than that of steady flows due to the fact that unsteady-flow conditions can change in relation to both. Ishak.et al. [10] studied the unsteady flow over a continuous stretching sheet. Theoretical investigation of the magnetohydrodynamically influenced viscous unsteady flow of a conducting fluid past a permeable stretched surface is carried out by Choudhary et al. [11]. Hafidzuddin et al. [12] examined the time dependent flow of a thick fluid over a permeable surface with a generalized slip velocity condition. Chaudhary et al. [13] investigated the magnetic field impact on unsteady flow of a viscous incompressible fluid's heat transfer process over a continuous stretched permeable surface. Qasim and Noreen [14] examined the heat transfer analysis of a Casson fluid over a permeable unsteady shrinking sheet with viscous dissipation present. Chamkha et al. [15] investigated the effects of heat and mass transfer on unsteady viscous flow past a permeable sheet embedded in a porous medium. The authors [15] found that the fluid flow significantly affected in presence of permeability, unsteadiness and chemical reaction parameters. Ramana et al. [16] explored the effects of a magnetic field and radiation on the time-dependent flow over a permeable stretched sheet, considering the effects of chemical reactions and multiple slips.

The book by Das et al. [17] covers a vast amount of literature on the subject of nanofluids. The first paper on stretching sheet for a nanofluid was presented by Khan and Pop [18]. The boundary layer flow of a time dependent heat transfer flow of a nanofluid over a permeable sheet is investigated by Bachok [19]. Elgazery [20] analysed the nanofluid flow across a permeable sheet with non-uniform heat source/sink and inclined magnetic field. In their study [20], the authors used four types of nanoparticles, including silver, copper, alumina, and titanium oxide, and found that the maximum (minimum) temperature is observed when titanium oxide (silver) nanoparticles are added to the base fluid water. Madhu et al. [21] studied the two-dimensional flow of a conducting non-Newtonian upper convicted Maxwell (UCM) nanofluid fluid over an unsteady permeable stretching sheet. Mjankwi et al. [22] examined the magnetohydrodynamic viscous nanofluid flow over an inclined permeable surface in the presence of heat and mass transfer effects. Khan et al. [23] studied the multiple slip effects on unsteady magnetohydrodynamic visco-elastic Jeffrey fluid model for buoyant nanofluid over a permeable sheet with thermal diffusion and radiation. The stagnation point flow (SPF) of a water-based hybrid nanofluid over a radially permeable shrinking or stretching surface is investigated by Khan et al. [24]. The authors noticed the dual solutions for shrinking and stretching cases. Analysing the flow of heat and mass transfer for Aluminium oxide, Copper, Silver, and Titanium oxide nanoparticles under the impact of a uniform magnetic field over a permeable linear stretching surface immersed in a porous medium was considered by Muntazir et al. [25]. The authors concluded that the flow rate is controlled by increasing the values of unsteady and suction/injection factors. Adnan et al. [26] examined the thermal performance of nanofluids for unsteady flow over a stretching surface. Azam Khan et al. [27] explores the magnetohydrodynamic stagnation point flow of a hybrid nanofluid flow consisting of alumina, copper, and water over a heated permeable stretching sheet. A lot of effort has been done exploring and investigating various physical geometries, with some research found in [28-35], due to the increasing demand of nanofluids in science and technology.

Suspension or dispersion of nano-material of high thermal conductivities into base fluid gives rise to higher thermal conductivity of the mixture, consequently, the heat transfer coefficient is raised. Because of their smaller size and larger interface area, nanoparticles stay suspended, which minimizes clogging and erosion. Several studies have shown that the thermal properties of base fluids can be dramatically altered by stable suspensions of a small amount of nanoparticles (1-5 vol.%) in conventional fluids. Stable nanofluids have been demonstrated to possess distinctive features, like high thermal conductivities at extremely low concentrations of nanoparticles [36-37], a nonlinear correlation between the concentration of particles and thermal conductivity [38–40], size-dependent conductivity and strong temperature [17& 41-42] and a critical heat flux in pool boiling that is, three times higher than to base fluids. Heat transfer fluids like propylene glycol/water are crucial to many industrial advancements, including power generation, chemical processing, central heating or preservation, and microelectronics [43]. According to Choi and Eastman [38], at volume fractions of 5% and 20%, respectively, the thermal conductivity of copper nanoparticles suspended in

water was increased by a factor of 1.5 and 3.5 when compared to water; this is significantly higher than the values observed for particles that were milli- or micro-meter sized. Yashawantha et al. [44] examined the rheological behavior and thermal conductivity of graphite-ethylene glycol (EG) nanofluid. When compared to nanoparticle size <100 nm, they discovered that the thermal conductivity increased by 16.3% for 2 vol.% nanofluid containing nanoparticles smaller than 50 nm. Further, the rheological behavior of water-based Al_2O_3 and TiO_2 nanofluids at various concentrations (0.1–2.0%) and temperatures between 293K–333K was also examined by the authors Das et al. [45]. They concluded that the Nanofluid also appears as a non-Newtonian fluid with a shear rate between 12 and $232s^{-1}$ as they exhibit shear thickening behavior. Saleh et al. [46] conducted an experimental investigation on the thermal efficiency, collector area, embodied energy, weight, and environmental CO_2 emissions of a Al_2O_3 water nanofluid above a flat-plate solar collector and with coiled wire turbulators. The readers can find the recent investigations in [47-50].

Natural or free convection can only happen when buoyancy forces are present. Here, it is important to note that forced convection transfers heat at a faster rate than free convection. Free convection, which is responsible for the natural circulation in flow loops, is essential for nuclear plant shutdown. In recent years, lots of studies on free convection flow have been published. Subba Reddy and Ibrahim [51] investigated the free convection flow of a viscous fluid over a vertical stretching sheet in presence of suction/injection. Rashidi et al. [52] examined the free convection MHD flow of a fluid over a permeable vertical stretching sheet with heat and mass transfer effects. Afify et al. [53] studied the slip effects, Newtonian heating, and radiation effects on boundary layer flow over a permeable sheet under the impact of magnetic field. Hasan et al. [54] concentrated on the analysis of magnetohydrodynamic free convection flow over a permeable inclined stretching sheet in presence of viscous dissipation and thermal radiation. The transient magnetohydrodynamics convection flow of a nanofluid across a porous permeable vertical stretching sheet was noticed by Freidoonimehr et al. [55]. The authors [55] developed the flow model by considering four different nanoparticles namely, copper, copper oxide, Aluminium oxide and titanium dioxide with water as base fluid.

The novelty of this study lies in its focus on water-based nanofluid with magnetic field, radiation, heat source/sink, viscous dissipation, and free convection, solved using the MATLAB bvp4c solver, which, to the best of the author's knowledge, has not been explored previously. Under the influence of the aforementioned effects, the current study has important practical applications, especially in the field of thermal-energy storage systems. These systems play a crucial role in gathering and storing excess thermal energy from various sources, including solar power and industrial processes, so that it can be used later on. Through an understanding of the intricate characteristics of nanofluids, phase change materials, and the effects of stretching/shrinking surfaces, researchers can optimize the thermal management performance, operational efficiency, and energy storage capacity of these systems [56]. Numerous practical applications for nanofluids exist, such as microelectronics, fuel cells, thermonuclear devices, biomedicine, and conveyance systems [57–61] (Table 1, 2).

The paper is structured into 6 sections. In section 1, the prior supported investigation to the present work is presented. In section 2, we formulate the flow model under the assumptions. In section 3, the constant and variable fluid characteristics are discussed. The numerical approach and results on various flow quantities are presented and analysed in sections 4 and 5. The concluding remarks are outlined at the end in section 6.

PROBLEM FORMULATION

The boundary layer incompressible flow of a two-dimensional, water based nanofluid across a porous material while thermal radiation, viscous dissipation, heat absorption/generation are taken into account. The time dependent magnetic field of strength B_0 with $B(x,\ t) = \frac{B_0}{\sqrt{(1-\lambda t)}}$ is used normal to the flow direction. The co-ordinate system and flow pattern are shown in Figure 1. The coefficient of porous permeability parameter and heat generation parameter is defined as $K'(x, t) = K_0\ (1 - \lambda t)$ and $Q^* = \frac{Q_0}{(1-\lambda t)}$ respectively. The thermal Grashoff number and velocity of the sheet is assumed as $g^* = \frac{g}{(1-\lambda t)^{\frac{3}{2}}}$ and $u_w(x,\ t) = \frac{cx}{(1-\lambda t)}$. Two distinct nanoparticle types Copper and Aluminum oxide with water are considered. The combination of Al_2O_3 and Cu nanoparticles in water is chosen to capitalize on their respective thermal properties, create synergies that improve heat transfer capabilities, potentially improve magnetohydrodynamic responses, and

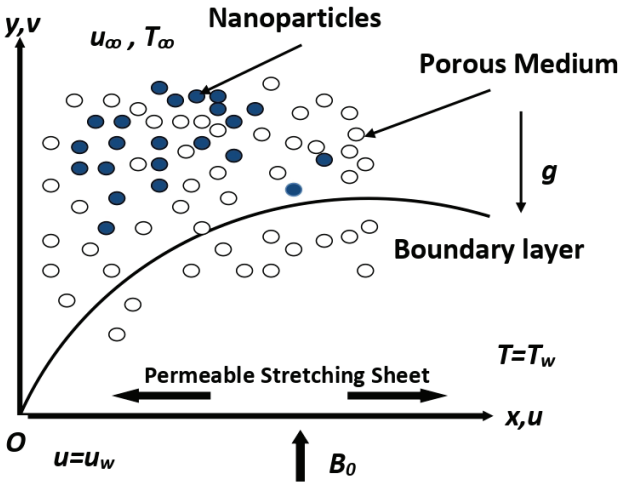

Figure 1. Geometric model.

maintain stability in practical applications. This combination represents a significant advancement in nanofluid technology, particularly in magnetohydrodynamics and heat transfer applications.

The present flow model is based on the following assumptions.

i. Due to a small magnetic Reynolds number and zero electric field, the induced magnetic field is supposed to be insignificant.
ii. Viscous dissipation, heat source/sink, and radiation have been considered.
iii. The sheet has been kept at constant wall temperature T_0 and T_∞ refers to the ambient temperature.
iv. Two equal and opposite forces lead the flow due to stretching or shrinking of the sheet from the origin.
v. Fluid is considered to be gray, absorbing but non-scattering medium that emits radiation.
vi. The radiation heat flow is described in the energy equation using the Rosseland approximation.
vii. The radiative heat flux is ignored in Y-axis.
viii. The base fluid and nanoparticles remain at state of thermal equilibrium.
ix. Nanoparticles are uniformly sized (1–100 nm) and have a spherical shape.
x. Thermal buoyancy force is often assumed to be used as a solution to thermal stratification.
xi. The volume fraction parameter's range of consideration is $0 < \phi \leq 0.1$.

Assuming the aforementioned, the time-dependent equations regulating the boundary layer are given by equations (1)- (3).

$$u_x + v_y = 0 \tag{1}$$

$$u_t + uu_x + vu_y = \nu_{nf} u_{yy} - \frac{\sigma_{nf}}{\rho_{nf}} B^2(x,t)u - \frac{\nu_{nf}}{K'(x,t)}u + g^* \frac{(\rho\beta)_{nf}}{\rho_{nf}}(T - T_\infty) \tag{2}$$

$$T_t + uT_x + vT_y = \alpha_{nf} T_{yy} + \frac{\mu_{nf}}{(\rho c_p)_{nf}} (u_y)^2 + \frac{1}{(\rho c_p)_{nf}} \left(\frac{16T_\infty^3 \sigma^*}{3K^*}\right) T_{yy} + \frac{Q^*}{(\rho c_p)_{nf}}(T - T_\infty) \tag{3}$$

The boundary conditions in linear permeable stretching sheet problems are pivotal in shaping the flow dynamics and heat transfer processes, and the overall physical interpretation of results. They provide the necessary constraints and context for mathematical models, ensuring that theoretical predictions align with observed behaviors in practical applications. In the present analysis, we assumed the following boundary conditions:

$$u = u_w = \frac{cx}{(1-\lambda t)}, v = v_w, T = T_w \; at \; y = 0 \text{ and } u \to 0, T \to T_\infty \text{ as } y \to \infty. \tag{4}$$

Solution of the Problem

The appropriate similarity transformations are

$$\psi = \sqrt{\frac{\upsilon c}{(1-\lambda t)}}\; x f(\eta), \eta = \sqrt{\frac{c}{\upsilon(1-\lambda t)}}\; y$$
$$u = \frac{\partial \psi}{\partial y} = \frac{cx\, f'(\eta)}{(1-\lambda t)}, v = -\frac{\partial \psi}{\partial x} = -\left[\sqrt{\frac{\upsilon c}{(1-\lambda t)}}\; f(\eta)\right], \tag{5}$$
$$\theta(\eta) = \frac{(T - T_\infty)}{(T_w - T_\infty)}$$

Where the wall temperature $T_w = T_\infty + \frac{bx}{(1-\lambda t)^2}\theta(\eta)$

In view of the similarity transformations the dimensionless ODE's and associated boundary conditions are given by equations (6)- (8).

$$f''' - (1-\phi)^{2.5} D_3 M f' - K f' + G_r (1-\phi)^{2.5} D_2 \theta - (1-\phi)^{2.5} D_1 \left[A\left(f' + \frac{\eta}{2} f''\right) + (f')^2 - f f''\right] = 0 \tag{6}$$

$$\frac{1}{D_4}\left[\frac{1}{Pr}\left(D_5 + \frac{4}{3}R\right)\theta'' + \frac{E_c (f'')^2}{(1-\phi)^{2.5}} + Q\theta\right] - A\left(2\theta + \frac{\eta\theta'}{2}\right) - f'\theta + \theta' f = 0 \tag{7}$$

The changed non-dimensional boundary conditions are

$$f = v_0, f' = 1, \theta = 1 \text{ at } \eta = 0$$
$$f' \to 0, \theta \to 0 \text{ as } \eta \to \infty \tag{8}$$

Where, $K = \frac{\nu_f}{cK_0}$, $M = \frac{\sigma_f B_0^2}{c\rho_f}$, $A = \frac{\lambda}{c}$, $G_r = \frac{g^* \beta_f b}{c^2}$, $Ec = \frac{u_w^2}{(T_w - T_\infty)c_{pf}}$, $Pr = \frac{(\mu c_p)_f}{k_f}$, $R = \frac{4\sigma^* T_\infty^3}{k_f k^*}$, $Q = \frac{Q_0}{C(\rho c_p)_f}$, $v_0 = \frac{-v_w}{\sqrt{\frac{\upsilon c}{(1-\lambda t)}}}$.

Here v_0 is the suction/injection parameter and $v_0 > 0$, $v_0 < 0$, and $v_0 = 0$ corresponds to suction, injection and impermeability cases respectively.

Table 1. The nanofluids' thermophysical characteristics [59, 60]

Physical property	Nanofluid
Viscosity (μ)	$\frac{\mu_f}{(1-\phi)^{2.5}}$
Density (ρ)	$(1-\phi)\rho_f + \phi\rho_s$
Heat capacity (ρc_p)	$(1-\phi)(\rho c_p)_f + \phi(\rho c_p)_s$
Thermal conductivity (k)	$\frac{(2k_f + k_s) + 2\phi(k_s - k_f)}{((2k_f + k_s) + \phi(k_f - k_s))} k_f$
Electrical conductivity (σ)	$\frac{(2\sigma_f + \sigma_s) + 2\phi(\sigma_s - \sigma_f)}{(2\sigma_f + \sigma_s) + \phi(\sigma_f - \sigma_s)} \sigma_f$
Diffusivity (α)	$\frac{k_{nf}}{(\rho c_p)_{nf}}$
Thermal Expansion ($\rho\beta$)	$(1-\phi)(\rho\beta)_f + \phi(\rho\beta)_s$

Table 2. The base fluid and nanoparticle's thermophysical properties [61]

Property	Copper (*Cu*)	Aluminium oxide (Al_2O_3)	Water (H_2O)
Density (ρ)	8,933	3,970	997.1
Specific heat (c_p)	385	765	4,179
Thermal conductivity (k)	401	40	0.613
Electrical conductivity (σ)	5.96×10^{7}	3.69×10^{7}	5.5×10^{-6}
Thermal expansion coefficient (β)	1.67×10^{-5}	0.85×10^{-5}	21×10^{-5}

Physical Quantities

Specific physical quantities of importance include the local skin-friction coefficient (C_f) and the local Nusselt number (Nu_x) are characterized as

$$C_f = \frac{\tau_w}{\rho_f u_w^2} \text{ and } Nu_x = \frac{x q_w}{k_f(T_w - T_\infty)}$$

Where

$$\tau_w = \mu_{nf}\left(\frac{\partial u}{\partial y}\right)_{at\ y=0} \text{and } q_w = -k_{nf}\left(\frac{\partial T}{\partial y}\right)_{at\ y=0}$$

$$C_f\sqrt{Re_x} = \frac{f''(0)}{(1-\phi)^{2.5}}, \text{ and}$$

$$(Re_x)^{-1/2}Nu_x = -\theta'(0).\frac{k_{nf}}{k_f} = -D_5\theta'(0)$$

Where $Re_x = \frac{u_w x}{\nu_f}$.

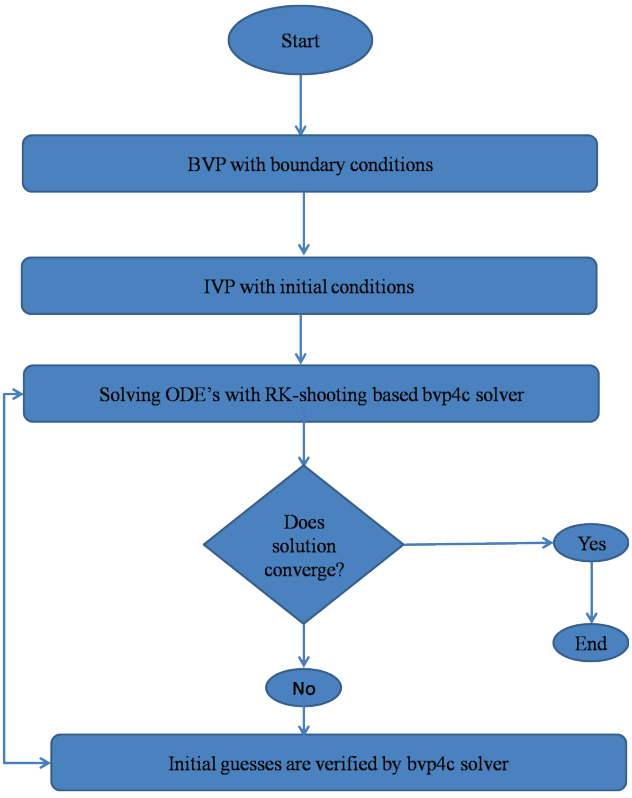

Figure 2. MATLAB simulation process.

Method of Solution

With the help of the powerful boundary value solver MATLAB bvp4c technique [62, 63], the set of non-linear ordinary differential equations (6)–(7) related to the boundary conditions (8) are numerically solved. However, using it requires some practice, and the tasks to be solved require some preliminary preparation, particularly when dealing with eigenvalue problems. This method is typically a collocation of order four, which includes the Runge-Kutta fourth-order shooting technique. The residual of the continuous solution is used to prepare the mesh choice and error mechanism. In the current problem, the decision of $\eta_\infty = 2$ ensures that each numerical solution approaches the asymptotic value accurately. The detailed MATLAB simulation process is explained in the Figure 2.

RESULTS AND DISCUSSION

In this section, the obtained results are presented and analysed for various flow parameters in Figures 3-15 and Table 3. The following parameter values have been fixed throughout our analysis $Ec = 0.5$, $\eta = 0.01$, $A = 0.5$, $Gr = 15$, $Pr = 6.2$ (*Water*), $M = 0.5$, $K = 0.5$, $R = 0.5$, $Q = 2$, $v_0 = 0.5$. Further, the results are discussed in two cases (i). Copper water nanofluid and (ii). Aluminium oxide water nanofluid.

In the absence of various effects of the current investigation, the numerical results are compared with the existed results of Ishak et al. [10] and Alrihieli et al. [64], and are depicted in Table 4. It is noticed that the current results are found to be in excellent agreement. The validity of the present results demonstrates the accuracy of the present method we used in the present study. The results are compared for the cases of suction ($v_0 > 0$), injection ($v_0 < 0$) and impermeability of the sheet ($v_0 = 0$).

The influence of magnetic field parameter (M) on fluid velocity for copper and aluminium water nanofluid is depicted in Figure 3. From this figure, it is seen that the fluid velocity decreases with an increasing values of M. For the simple reason that Lorentz force gets stronger as M increases, hence retarding the velocity. Furthermore, the significant reduction is observed on Copper-water nanofluid. The impact of the porous permeability parameter (K) on velocity filed is presented in Figure 4. It is noticed that the fluid velocity is a decreasing function of K. Physically, an increase in K causes to amplifies the porous layer.

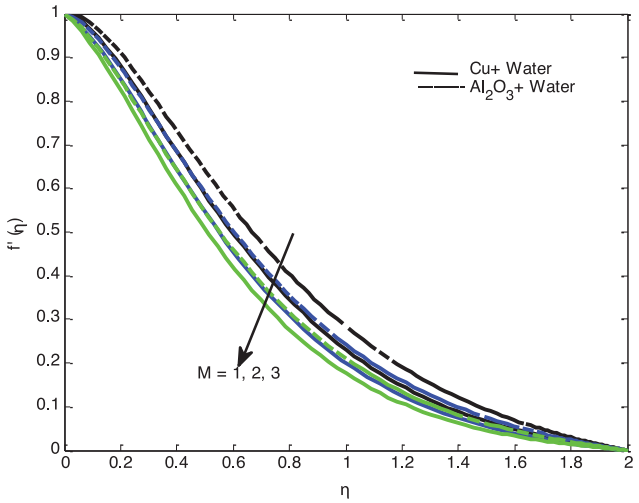

Figure 3. Impact of M on $f'(\eta)$.

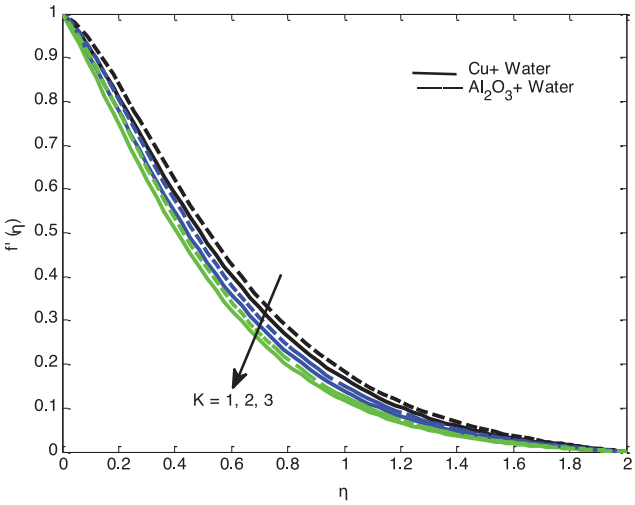

Figure 4. Impact of K on $f'(\eta)$.

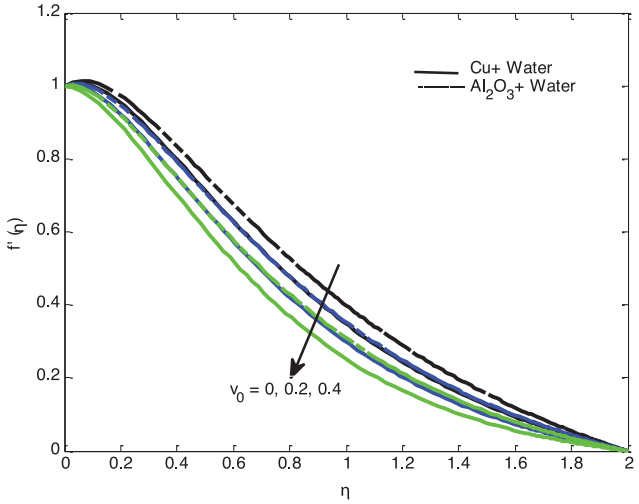

Figure 5. Impact of v_0 on $f'(\eta)$.

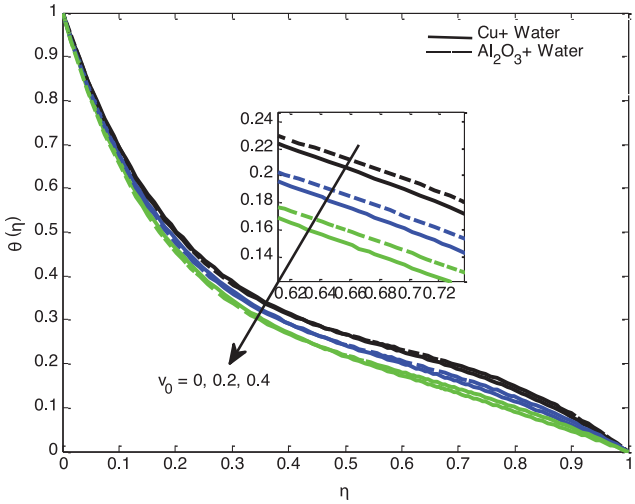

Figure 6. Impact of v_0 on $\theta(\eta)$.

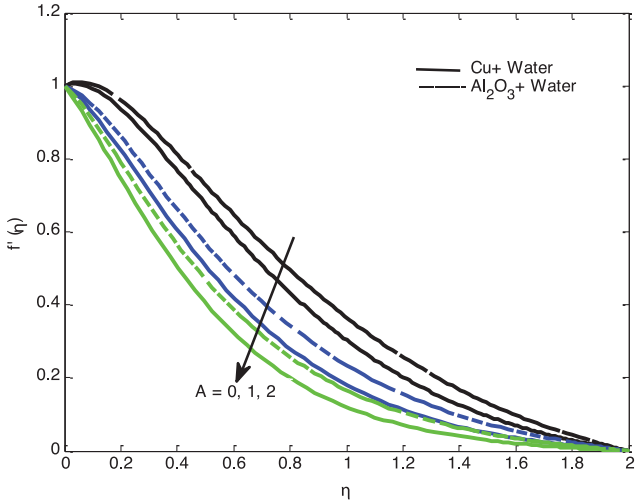

Figure 7. Impact of A on $f'(\eta)$.

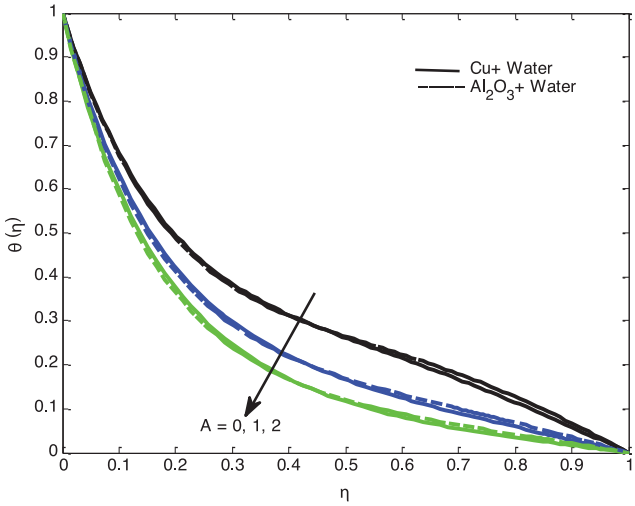

Figure 8. Impact of A on $\theta(\eta)$.

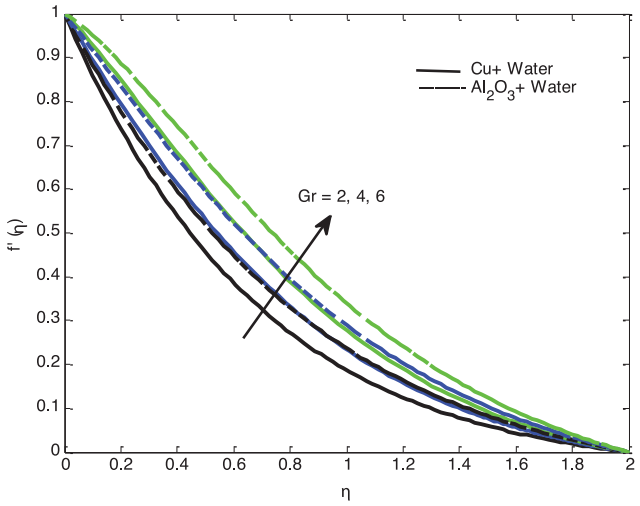

Figure 9. Impact of Gr on $f'(\eta)$.

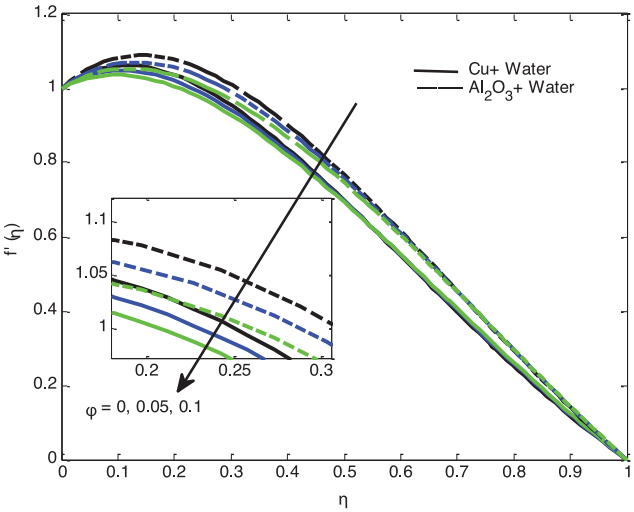

Figure 10. Impact of ϕ on $f'(\eta)$.

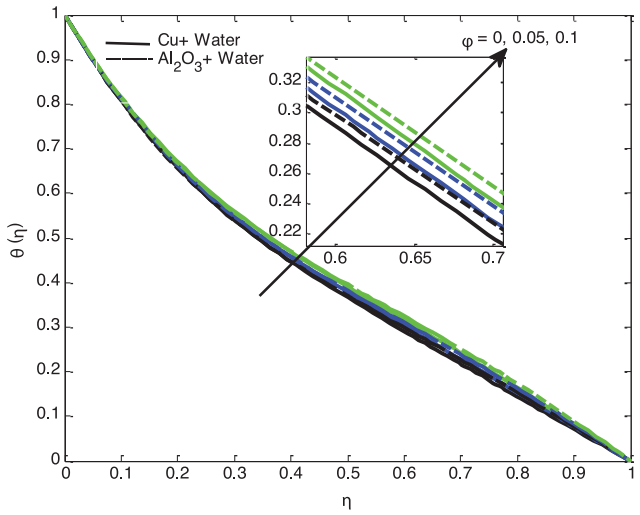

Figure 11. Impact of ϕ on $\theta(\eta)$.

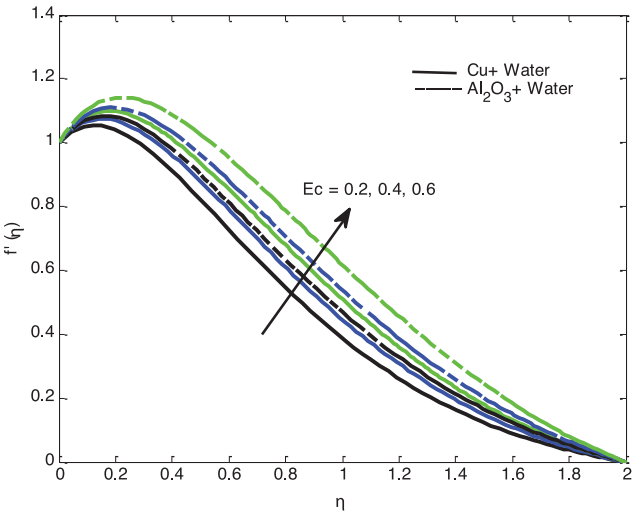

Figure 12. Impact of Ec on $f'(\eta)$.

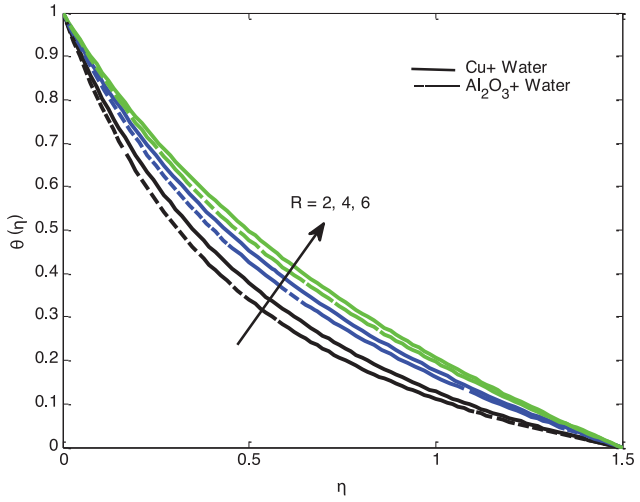

Figure 13. Impact of R on $\theta(\eta)$.

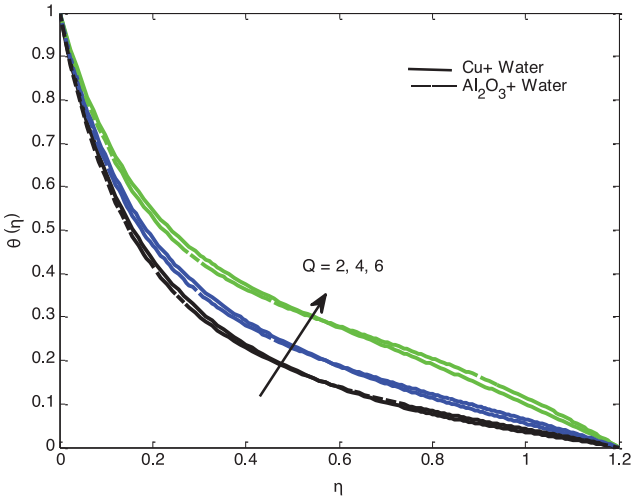

Figure 14. Impact of Q on $\theta(\eta)$.

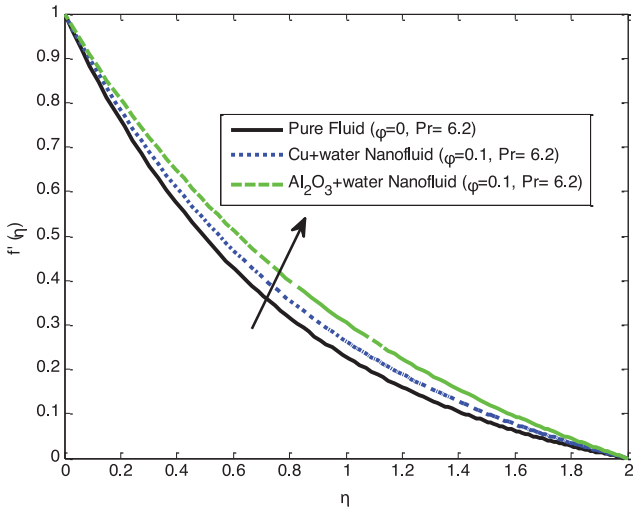

Figure 15. Comparison between velocity of nanofluids and pure fluids.

Therefore, the fluid velocity is reduced. The effect of suction parameter v_0 on velocity and temperature fields is illustrated in Figures 5-6. From the figures, it is noticed that, the velocity and temperature profiles of copper water and aluminium water nanofluid reductions with a growing values of v_0. This is because the presence of suction could increase the flow resistance. Additionally, the same trend is noticed for the temperature field. Further, these profiles show the significant behavior on copper water nanofluid. Figures 7 and 8 reflects the influence of unsteadiness parameter (A) on velocity and temperature fields. The Figures 7 and 8 shows decreasing behavior of velocity and temperature for higher values of A. Dissimilar behavior is seen in the temperature profiles, with the nanofluids' temperature decreasing at the surface and then increasing with a larger estimate of unsteadiness. Moreover, unsteadiness causes to reduce the thickness of momentum and thermal boundary layer. Impact of unsteadiness is dominant near the sheet.

Table 3. Numerical values of $Re_x^{1/2}C_f$, and $Re_x^{-1/2}N_u$, for various values of flow parameters when $\phi = 0.1$, $\eta = 0.01$, $Ec = 0.5$, $v_0 = 0.5$, $Pr = 6.2$, $A = 0.5$, $Gr = 15$, $R = Q = 0.2$, $M = K = 0.5$

M	K	A	Gr	v_0	R	Q	Ec	$Re_x^{1/2}\,C_f$		$(Re_x)^{-1/2}\,N_{u_x}$	
								$Cu+H_2O$	$Al_2O_3+H_2O$	$Cu+H_2O$	$Al_2O_3+H_2O$
0.1								0.465343	0.685064	5.063098	5.149823
0.2								0.431585	0.647279	5.051441	5.139308
0.3								0.398238	0.610093	5.039557	5.128427
	0.1							0.526625	0.754036	5.083281	5.167574
	0.2							0.476843	0.697968	5.066982	5.153287
	0.3							0.427960	0.643230	5.050167	5.138149
		1						-0.245573	0.027764	5.585690	5.716979
		2						-1.089287	-0.710031	6.440126	6.647265
		3						-1.724004	-1.263202	7.124130	7.395142
			0					-2.721362	-2.353591	3.108954	3.509238
			5					-1.653568	-1.348202	4.076843	4.339964
			10					-0.648293	-0.395611	4.685926	4.851405
				0				0.965320	1.109451	3.895986	3.891532
				0.2				0.733684	0.893043	4.341410	4.368195
				0.4				0.473579	0.659982	4.790860	4.857488
					2			1.225049	1.452637	2.925403	2.911054
					4			1.730857	1.971222	2.171792	2.138600
					6			2.037183	2.285339	1.797449	1.760449
						0.1		0.368923	0.572777	4.933734	5.023251
						0.2		0.332723	0.537412	5.015163	5.105667
						0.3		0.298013	0.503557	5.094738	5.186136
							0.2	-0.048744	0.185882	5.331050	5.365611
							0.4	0.213540	0.427802	5.096955	5.173899
							0.6	0.444177	0.639694	4.950629	5.050474

Table 4. Comparison of Nusselt number $-\theta'(0)$. for various values of v_0 and Pr with the results of Ishak et al. [10] and Alrihieli et al. [64] when $\phi = 0$, $Ec = 0$, $A = 0$, $Gr = 0$, $M = 0$, $R = 0$, $K = 0$ and $Q = 0$

Pr	v_0	Ishak et al. [10]	Alrihieli et al. [64]	Present Work
0.72	-1.5	0.4570	0.457001520	0.457153
1.0	-1.5	0.5000	0.500000000	0.500005
10	-1.5	0.6542	0.654211910	0.645161
0.72	0.0	0.8086	0.808589088	0.808681
1.0	0.0	1.0000	1.000000000	1.000001
3.0	0.0	1.9237	1.923689985	1.923677
10.0	0.0	3.7207	3.720699510	3.720591
0.72	1.5	1.4944	1.494389791	1.494567
1.0	1.5	2.0000	2.000002010	2.000008
10	1.5	16.0842	16.08419892	16.084199

Figure 9 depicts the velocity profiles for distant values of thermal Grashof number (Gr). It is seen that the velocity profiles improved for growing values of Gr in both cases. Also, higher velocity is observed for Aluminium oxide nanofluid. This is due to the fact that, positive values of Gr works as a suitable pressure gradient to accelerate the momentum boundary layer. Figure 10 shows the effect of volume fraction parameter (ϕ) on fluid velocity. It is seen that the boundary layer thickness drops with the rising values of ϕ. This is because increasing the volume fraction parameter ϕ causes the fluid's velocity to increase, which in turn increases viscous forces and causes the velocity of the fluid to decrease. Moreover, for base fluid ($\phi = 0$) higher velocity is observed near the sheet, later it decreases with mixing nanoparticles into the base fluid. While the reverse trend is noticed on temperature field (Figure 11). Figure 12 shows that the nanofluid velocity is enhanced for rising values of Eckert number (Ec). The reason is raising values of Ec causes the faster nanoparticle movement in the fluids and the dissipation of some kinetic energy through viscosity. The effect of thermal radiation (R) on fluid temperature is displayed on Figure 13. In both cases, it is seen that the nanofluid's temperature rises as a function of R. This indicates that a hotter body emits radiation with a higher intensity. Compared to aluminum water nanofluid, copper water nanofluid has a thicker thermal boundary layer. From Figure 14, it is clear that the fluid temperature is an increasing function of heat source parameter (Q) Physically, heat generation phenomenon creates an enhancement in the transfer and thermal spread of fluids, which leads to raise in temperature of the fluid. In addition, a high temperature for the copper water nanofluid is observed nearer to the sheet. Later, aluminium oxide temperature dominates the Copper water nanofluid. The comparison results of velocity for base fluid, Copper water nanofluid and Aluminium water nanofluid is presented in Figure 15. The figure shows that on mixing the nanoparticles into the water, the fluid velocity is significantly increased. This is because of the significant thermal conductivity, enhanced convective heat transfer, high surface area-to-volume ratio compared to the base fluid molecules and Stability and Suspension of nanoparticles.

The numerical results of the coefficient of Skin friction and Nusselt number for two cases against various flow parameters are displayed in Table 3. From this table, as the values of M, K, A, v_0 and Q increase, it is evident that the friction near the wall reduces in both cases. Since the friction is caused when a fluid rubs against the surface of an element moving through it. While it increases for Gr, R and Ec. Due to the fact that it is proportionate to the area of the surface in contact with the fluid and grows with the square of the velocity. Further, the improving values of flow quantities A, Gr, v_0 and Q causes to develop the heat transfer rate for both nanofluids. But the opposite trend is noticed for the flow parameters M, K, R and Ec. The appropriate diffusion of nanomaterials in the base fluid is made possible by the behavior of the atomic chain, which offers significant advantages like increased heat conduction, reduced possibilities of erosion, improved thermal conductivity, and mixture stability. Throughout the analysis, Skin friction and Nusselt number results for Aluminium water nanofluid plays a dominant role than the Copper water nanofluid.

CONCLUSION

An unstable MHD free convection flow of a water based nanofluid past a permeable linearly stretched sheet through a porous medium is studied to determine the influence of heat transfer effects. The MATLAP bvp4c solver is used to numerically solve the collection of linked ODEs. The results are discussed and illustrated using graphs and tables.

The main outcomes in this investigation include

1. When both magnetic field strength and porosity are increased simultaneously, their combined effects synergistically decrease the fluid velocity. The magnetic field acts directly on the nanoparticles, affecting their

behavior and interactions within the fluid. Concurrently, the porous medium introduces additional resistance and alters the flow dynamics, compounding the overall decrease in velocity.

2. The suction parameter reduces the fluid velocity field because it decreases the amount of fluid entering the system, thereby impacting both the temperature distribution and the velocity profiles within the flow domain. This understanding is crucial in various engineering applications where suction or injection is used to control flow characteristics and heat transfer rates.
3. Because of the significant thermal conductivity, enhanced convective heat transfer, high surface area, Stability and Suspension of nanoparticles, the nanofluids exhibiting superior heat transfer performance compared to their base fluids, making them attractive options for various heat transfer applications such as cooling systems, heat exchangers, and thermal management in electronics.
4. As radiation and heat source parameters increase, the thermal and velocity fields within the boundary layer adjust to accommodate the increased heat transfer and energy distribution. These adjustments lead to changes in velocity gradients, viscosity, and ultimately frictional forces at the wall.
5. A significant phenomenon on nanofluid velocity is noticed for greater unsteadiness parameter values.
6. The Grashof number and viscous dissipation parameters improved the fluid velocity.

NOMENCLATURE

B_0 Uniform Magnetic field strength
T Temperature of the fluid
ρ Density of fluid
M Magnetic field parameter
Pr Prandtl number
R Thermal radiation Parameter
g Acceleration due to gravity
Gr Grashof number
Q_0 Heat source/sink coefficient
Q Heat source/sink parameter
Ec : Eckert number
k Thermal conductivity
q_r Radiative heat flux
A Unsteadiness Parameter
v_0 Suction/Injection parameter
K' Porous permeability
K_0 : Permeability constant
K Porous Permeability parameter
q_w Heat flux
K^* Mean absorption coefficient
Re_x Reynolds number
u,v Components of velocity in the x and y directions
t Time
f Non-dimensional stream function
b,c Constants

Greek symbols
ψ Dimensional Stream function
τ Shear stress
$\sigma\hat{}*$ Stefan-Boltzman constant
α Thermal diffusivity
β Thermal expansion coefficient
σ Electrical conductivity
η Similarity variable
θ Non-dimensional temperature
ϕ Volume fraction of nanoparticles
λ Parameter
μ Coefficient of viscosity
ν Kinematic viscosity

Subscripts
nf Nanofluid
f Base fluid
w Condition on the wall
∞ Ambient condition

Superscripts
' Differentiation w.r.t η.

Abbreviations
BVP Boundary Value problem.
IVP Initial Value problem.
ODE Ordinary Differential Equation.
PDE Partial Differential Equation.
Cu Copper Nanoparticle.
Al_2O_3 Aluminium oxide Nanoparticle.
MHD Magnetohydrodynamics.

AUTHORSHIP CONTRIBUTIONS

Authors equally contributed to this work.

DATA AVAILABILITY STATEMENT

The authors confirm that the data that supports the findings of this study are available within the article. Raw data that support the finding of this study are available from the corresponding author, upon reasonable request.

CONFLICT OF INTEREST

The authors declared no potential conflicts of interest with respect to the research, authorship, and/or publication of this article.

ETHICS

There are no ethical issues with the publication of this manuscript.

REFERENCES

[1] Sakiadis BC. Boundary-layer behavior on continuous solid surfaces: I. Boundary-layer equations for two-dimensional and axisymmetric flow. AIChE J 1961;7:26–28. [CrossRef]

[2] Sakiadis BC. Boundary-layer behavior on continuous solid surfaces: II. The boundary layer on a continuous flat surface. AIChE J 1961;7:221–225. [CrossRef]

[3] Crane LJ. Flow past a stretching plate. Z Angew Math Phys 1970;21:645–647. [CrossRef]

[4] Gupta PS, Gupta AS. Heat and mass transfer on a stretching sheet with suction or blowing. Can J Chem Eng 1977;55:744–746. [CrossRef]

[5] Pop I, Tsung-Yen Na. A note on MHD flow over a stretching permeable surface. Mech Res Commun 1998;25:263–269. [CrossRef]

[6] Kumaran V, Banerjee AK, Vanav Kumar A, Vajravelu K. MHD flow past a stretching permeable sheet. Appl Math Comput 2009;210:26–32. [CrossRef]

[7] Ali FM, Nazar, Norihan Md Arifin. MHD viscous flow and heat transfer induced by a permeable shrinking sheet with prescribed surface heat flux. WSEAS Trans Math 2010;9:365–375.

[8] Hayat T, Qasim M, Mesloub S. MHD flow and heat transfer over a permeable stretching sheet with slip conditions. Int J Numer Methods Fluids 2011;66:963–975. [CrossRef]

[9] Mabood F, Shateyi S. Multiple slip effects on MHD unsteady flow heat and mass transfer impinging on a permeable stretching sheet with radiation. Model Simul Eng 2019;2019:1–11. [CrossRef]

[10] Ishak A, Nazar R, Pop I. Heat transfer over an unsteady stretching permeable surface with prescribed wall temperature. Nonlinear Anal Real World Appl 2009;10:2909–2913. [CrossRef]

[11] Choudhary MK, Chaudhary S, Sharma R. Unsteady MHD flow and heat transfer over a stretching permeable surface with suction or injection. Procedia Eng 2015;127:703–710. [CrossRef]

[12] Hafidzuddin MEH, Nazar RM, Arifin N, Pop I. Unsteady flow and heat transfer over a permeable stretching/shrinking sheet with generalized slip velocity. Int J Numer Methods Heat Fluid Flow 2018;28:1457–1470. [CrossRef]

[13] Chaudhary S, Chaudhary S, Singh S. Heat transfer in hydromagnetic flow over an unsteady stretching permeable sheet. Int J Math Eng Manag Sci 2019;4:1018–1030. [CrossRef]

[14] Qasim M, Noreen S. Heat transfer in the boundary layer flow of a Casson fluid over a permeable shrinking sheet with viscous dissipation. Eur Phys J 2014;129:1–8. [CrossRef]

[15] Chamkha AJ, Aly AM, Mansour MA. Similarity solution for unsteady heat and mass transfer from a stretching surface embedded in a porous medium with suction/injection and chemical reaction effects. Chem Eng Commun 2010;197:846–858. [CrossRef]

[16] Mohana Ramana R, Venkateswara Raju K, Girish Kumar J. Multiple slip and chemical reaction effects on unsteady MHD heat and mass transfer flow over a permeable stretching sheet with radiation. Turk J Comput Math Educ 2021;12:4489–4498.

[17] Das SK, Choi SU, Yu W, Pradeep T. Nanofluids: Science and Technology. New York: John Wiley & Sons Inc; 2008. pp. 344–345.

[18] Khan WA, Pop I. Boundary-layer flow of a nanofluid past a stretching sheet. Int J Heat Mass Transf 2010;53:2477–2483. [CrossRef]

[19] Bachok N, Ishak A, Pop I. Unsteady boundary-layer flow and heat transfer of a nanofluid over a permeable stretching/shrinking sheet. Int J Heat Mass Transf 2012;55:2102–2109. [CrossRef]

[20] Elgazery NS. Nanofluids flow over a permeable unsteady stretching surface with a non-uniform heat source/sink in the presence of an inclined magnetic field. J Egypt Math Soc 2019;27:9. [CrossRef]

[21] Madhu M, Kishan N, Chamkha AJ. Unsteady flow of a Maxwell nanofluid over a stretching surface in the presence of magnetohydrodynamic and thermal radiation effects. Propuls Power Res 2017;6:31–40. [CrossRef]

[22] Mjankwi MA, Masanja VC, Mureithi EW, MakunguNg'oga J. Unsteady MHD flow of nanofluid with variable properties over a stretching sheet in the presence of thermal radiation and chemical reaction. Int J Math Math Sci 2019;2019:1–14. [CrossRef]

[23] Khan SA, Nie Y, Ali B. Multiple slip effects on MHD unsteady viscoelastic nanofluid flow over a permeable stretching sheet with radiation using the finite element method. SN Appl Sci 2020;2:66. [CrossRef]

[24] Khan U, Waini I, Ishak A, Pop I. Unsteady hybrid nanofluid flow over a radially permeable shrinking/stretching surface. J Mol Liq 2021;331:115752. [CrossRef]

[25] Muntazir RM, Mushtaq M, Shahzadi S, Jabeen K. MHD nanofluid flow around a permeable stretching sheet with thermal radiation and viscous dissipation. Proc Inst Mech Eng Part C J Mech Eng Sci 2022;236:137–152. [CrossRef]

[26] Adnan UK, Ahmed N, Tauseef S, Mohyud Din, Alsulami MD, Khan I. A novel analysis of heat transfer in the nanofluid composed by nanodiamond and silver nanomaterials: numerical investigation. Sci Rep 2022;12:1284. [CrossRef]

[27] Khan AA, Zaimi K, Ying TY. Unsteady MHD stagnation point flow of Al_2O_3-Cu/H_2O hybrid nanofluid past a convectively heated permeable stretching/shrinking sheet with suction/injection. J Adv Res Fluid Mech Therm Sci 2022;96:96–114. [CrossRef]

[28] Kumar VG, Rehman KU, Kumar RVMSSK, Shatanawi W. Unsteady magnetohydrodynamic nanofluid flow over a permeable exponentially surface manifested with non-uniform heat source/sink effects. Waves Random Complex Media 2022;1–19. [CrossRef]
[29] Oyelakin IS, Mondal S, Sibanda P. Unsteady MHD three-dimensional Casson nanofluid flow over a porous linear stretching sheet with slip condition. Front Heat Mass Transf 2017;8:1–9. [CrossRef]
[30] Hymavathi T, Mathews J, Kumar RVMSSK. Heat transfer and inclined magnetic field effects on unsteady free convection flow of MoS_2 and MgO–water-based nanofluids over a porous stretching sheet. Int J Ambient Energy 2022;43:5855–5863. [CrossRef]
[31] Kumar RVMSS, Varma SVK. Multiple slips and thermal radiation effects on MHD boundary layer flow of a nanofluid through a porous medium over a nonlinear permeable sheet with heat source and chemical reaction. J Nanofluids 2017;6:48–58. [CrossRef]
[32] Khashi'ie NS, Waini I, Arifin NM, Pop I. Unsteady squeezing flow of Cu-Al_2O_3/water hybrid nanofluid in a horizontal channel with a magnetic field. Sci Rep 2021;11:14128. [CrossRef]
[33] Shahzad U, Mushtaq M, Farid S, Jabeen K, Muntazir RM. A numerical approach for an unsteady tangent hyperbolic nanofluid flow past a wedge in the presence of suction/injection. Math Probl Eng 2021;2021:1–15. [CrossRef]
[34] Shuaib M, Ali A, Khan MA, Ali A. Numerical investigation of an unsteady nanofluid flow with magnetic and suction effects to the moving upper plate. Adv Mech Eng 2020;12:1–13. [CrossRef]
[35] Ahamed SM, Mondal S, Sibanda P. Unsteady mixed convection flow through a permeable stretching flat surface with partial slip effects through MHD nanofluid using the spectral relaxation method. Open Phys 2017;15:323–334. [CrossRef]
[36] Eastman JA, Choi SUS, Li S, Yu W, Thompson LJ. Anomalously increased effective thermal conductivities of ethylene glycol–based nanofluids containing copper nanoparticles. Appl Phys Lett 2001;78:718–720. [CrossRef]
[37] Patel HE, Das SK, Sundararajan T, Sreekumaran NA, George B, Pradeep T. Thermal conductivities of naked and monolayer protected metal nanoparticle-based nanofluids: manifestation of anomalous enhancement and chemical effects. Appl Phys Lett 2003;83:2931–2933. [CrossRef]
[38] Choi SUS, Eastman JA. Enhancing thermal conductivity of fluids with nanoparticles. Am Soc Mech Eng 1995;66:99–105.
[39] Vassallo P, Kumar R, D'Amico S. Pool boiling heat transfer experiments in silica–water nanofluids. Int J Heat Mass Transfer 2004;47:407–411. [CrossRef]
[40] Li X, Zhu D, Wang X. Evaluation on dispersion behavior of the aqueous copper nano-suspensions. J Colloid Interface Sci 2007;310:456–463. [CrossRef]
[41] Chon CH, Kihm KD, Lee SP, Choi SUS. Empirical correlation finding the role of temperature and particle size for nanofluid (Al_2O_3) thermal conductivity enhancement. Appl Phys Lett 2005;87:153107. [CrossRef]
[42] Das SK, Putra N, Thiesen P, Roetzel W. Temperature dependence of thermal conductivity enhancement for nanofluids. J Heat Transf 2003;125:567–574. [CrossRef]
[43] Olabi AG, Wilberforce T, Sayed ET, Elsaid K, Atiqure Rahman SM, Abdelkareem MA. Geometrical effect coupled with nanofluid on heat transfer enhancement in heat exchangers. Int J Thermofluids 2021;10:100072. [CrossRef]
[44] Yashawantha KM, Asif A, Babu RG, Ramis MK. Rheological behavior and thermal conductivity of graphite–ethylene glycol nanofluid. J Test Eval 2021;49:2906–2927. [CrossRef]
[45] Das PK, Dash SK, Ganguly R, Santra AK, Venkatesan EP, Rajhi AA, Saboor S, et al. Effect of particle loading and temperature on the rheological behavior of Al_2O_3 and TiO_2 nanofluids. Energy Sources Part A Recover Util Environ Eff 2022;44:7062–7079. [CrossRef]
[46] Saleh B, Sundar LS, Aly AA, Venkata Ramana E, Sharma KV, Afzal A, et al. The combined effect of Al_2O_3 nanofluid and coiled wire inserts in a flat-plate solar collector on heat transfer, thermal efficiency, and environmental CO_2 characteristics. Arab J Sci Eng 2022;47:9187–9214. [CrossRef]
[47] Taghikhani MA. Magnetic field effect on the heat transfer in a nanofluid-filled lid-driven cavity with Joule heating. J Therm Eng 2020;6:521–543. [CrossRef]
[48] Thameem Basha H, Sivaraj R. Heat and mass transfer in stagnation point flow of cross nanofluid over a permeable extending/contracting surface: a stability analysis. J Therm Eng 2022;8:38–51. [CrossRef]
[49] Pattnaik PK, Syed SA, Mishra S, Swarnalata J, Sachindar Kumar R, Muduli K. Flow of viscous nanofluids across a nonlinear stretching sheet. J Therm Eng 2023;9:593–601. [CrossRef]
[50] Paul A, Mani Nath J, Das TK. An investigation of the MHD Cu-Al_2O_3/H_2O hybrid-nanofluid in a porous medium across a vertically stretching cylinder incorporating thermal stratification impact. J Therm Eng 2023;9:799–810. [CrossRef]
[51] Rama Subba Reddy G, Ibrahim S. Free convection on a vertical stretching surface with suction and blowing. Appl Sci Res 1994;52:247–257. [CrossRef]
[52] Rashidi MM, Rostami B, Freidoonimehr N, Abbasbandy S. Free convective heat and mass transfer for MHD fluid flow over a permeable vertical stretching sheet in the presence of radiation and buoyancy effects. Ain Shams Eng J 2014;5:901–912. [CrossRef]

[53] Afify AA, Uddin MJ, Ferdows M. Scaling group transformation for MHD boundary layer flow over a permeable stretching sheet in the presence of slip flow with Newtonian heating effects. Appl Math Mech 2014;35:1375–1386. [CrossRef]
[54] Hasan M, Karim E, Samad A. MHD free convection flow past an inclined stretching sheet considering viscous dissipation and radiation. Open J Fluid Dyn 2017;7:152–168. [CrossRef]
[55] Freidoonimehr N, Rashidi MM, Mahmud S. Unsteady MHD free convective flow past a permeable stretching vertical surface in a nanofluid. Int J Therm Sci 2015;7:136–145. [CrossRef]
[56] Lim YJ, Mohamad AQ, Rawi NA, Ling DCC, Zin NAM, Shafie S. Analysis of quadratic thermal radiation on Carreau fluid past a melting stretchable cylinder. Res Square 2023 Jan 05. [Preprint] [CrossRef]
[57] Wong KFV, Leon OD. Applications of nanofluids: current and future. Adv Mech Eng 2010;2:519659. [CrossRef]
[58] Barai D, Bhanvase BA. Future prospects of industrial applications of nanofluids. In: Bhanvase BA, Barai D, Zyla G, Said Z, eds.Towards Nanofluids For Large-Scale Industrial Applications. Amsterdam: Elsevier; 2024. pp. 429–446. [CrossRef]
[59] Gupta S, Kumar D, Singh J. Magnetohydrodynamic three-dimensional boundary layer flow and heat transfer of water-driven copper and alumina nanoparticles induced by convective conditions. Int J Mod Phys B 2019;33:1950307. [CrossRef]
[60] Das K, Sarkar A, Kumar PK. Cu-water nanofluid flow induced by a vertical stretching sheet in the presence of a magnetic field with convective heat transfer. Propuls Power Res 2017;6:206–213. [CrossRef]
[61] Oztop HF, Abu-Nada E. Numerical study of natural convection in partially heated rectangular enclosures filled with nanofluids. Int J Heat Fluid Flow 2008;29:1326–1336. [CrossRef]
[62] Ascher UM, Mattheij RMM, Russell RD. Numerical solution of boundary value problems for ordinary differential equations. Philadelphia: SIAM; 1995. [CrossRef]
[63] Shampine LF, Reichelt MW, Kierzenka J. Solving boundary value problems for ordinary differential equations in MATLAB with bvp4c. Available at: https://classes.engineering.wustl.edu/che512/bvp_paper.pdf. Accessed Feb 26, 2025.
[64] Alrihieli H, Alrehili M, Megahed AM. Radiative MHD nanofluid flow due to a linearly stretching sheet with convective heating and viscous dissipation. Mathematics 2022;10:4743. [CrossRef]

APPENDIX

$$D_1 = 1 - \phi + \phi \frac{\rho_s}{\rho_f}$$

$$D_2 = 1 - \phi + \phi \frac{(\rho\beta)_s}{(\rho\beta)_f}$$

$$D_3 = 1 - \phi + \phi \frac{\sigma_s}{\sigma_f}$$

$$D_4 = 1 - \phi + \phi \frac{(\rho c_p)_s}{(\rho c_p)_f}$$

$$D_5 = \frac{K_{nf}}{K_f} = \frac{(2K_f + K_s) - 2\phi(K_f - K_s)}{(2K_f + K_s) + \phi(K_f - K_s)}$$